Quantum chaos and a periodically perturbed Eberly-Chirikov pendulum

Ronald F. Fox and John Eidson
School of Physics, Georgia Institute of Technology, Atlanta, Georgia 30332
(Received 21 October 1985; revised manuscript received 18 February 1986)

A two-level system contained in a single-mode resonant cavity tuned to the energy-level separation of the two-level system is studied. A purely quantum-level description is converted into five coupled ordinary differential equations for certain relevant expectation values. These equations are identical with a system of equations proposed by Belobrov, Zaslavskii, and Tartakovskii on semiclassical grounds, and very closely related to a similar system proposed by Milonni, Ackerhalt, and Galbraith on semiclassical grounds. The level-population expectation value for the two-level system shows a transition to chaos as the coupling strength is increased. This transition is suggested by power spectra and confirmed by calculation of corresponding Liapunov exponents. It is shown that the equations can be transformed so that they exhibit the presence of a periodically perturbed Eberly-Chirikov pendulum as the key dynamical element responsible for the observed behavior. Numerical simulation of this periodically perturbed pendulum is shown to reproduce the peculiar features of the observed spectra obtained for the full, five-variable model. We discuss the relationship of these studies to the issue of *bona fide* chaos in a purely quantum-mechanical-level description of the system.

I. INTRODUCTION

In 1968, Eberly[1] showed that the dynamics of a two-level quantum system in a coherent radiation field is closely related to the dynamics of a classical spherical pendulum. At about the same time, Chirikov[2,3] and Zaslavskii showed that the deterministic dynamics near the separatrix of a classical, planar pendulum is stochastic in character. These facts suggested that a two-level quantum system interacting with its own radiation field in a resonant cavity might provide an example of a simple quantum system which can exhibit chaos.

Soon after we began our investigation of this possibility, we learned of the closely related study by Milonni, Ackerhalt, and Galbraith[4] (MAG) which in essence confirmed our expectation. They considered the semiclassical Jaynes-Cummings model[5] which has been greatly studied in the rotating-wave approximation (RWA). They showed that the terms neglected in the RWA lead to chaos when they are kept. The chaos was diagnosed from power spectra and confirmed by computation of Liapunov exponents.

An erratum[6] brought to our attention the earlier work of Belobrov, Zaslavskii, and Tartakovskii[7] (BZT) in which essentially the same system was studied and chaos was exhibited by phase-space trajectory plots and the exponential separation of initially close trajectories. They too showed that the chaos was a consequence of inclusion of terms normally neglected in the RWA.

In spite of these achievements, a number of important questions remained unanswered. The models studied by MAG and by BZT are not identical. Can this be explained starting from the fully quantum-mechanical description and deriving the semiclassical description? The spectra obtained by MAG for both the chaotic regime and the nonchaotic regime are quite peculiar looking (see Figs. 1 and 2). Can the major features of these spectra be explained? Can Eberly's spherical pendulum or Chirikov's planar pendulum be found explicitly in this system? In this paper, we answer each of these questions. We begin with the full quantum theory and show how to obtain the semiclassical theory as a consequence of factorization of nonlinear expectation values. We make an error estimate for the validity of this factorization. The result is identical to the BZT model. This is seen to be a consequence of the feedback effect of the two-level system on its own resonant radiation field. The feedback shows itself in the semiclassical theory as an effective current-density source rather than as an effective polarization density. This type of subtle distinction has been observed before, in a different context, by Mandel.[8] It is the basis for the subtle difference between the MAG model and the BZT model. By change of variables, we are able to show that Eberly's spherical pendulum is contained in the BZT model in the RWA. Moreover, the initial conditions used in the study of the BZT model imply that the constant corresponding to the azimuthal angular momentum of a spherical pendulum is precisely zero in the RWA. This reduces Eberly's pendulum to Chirikov's planar pendulum. In addition, the initial conditions imply that, at resonance, Chirikov's pendulum is operating very close to its separatrix in the RWA. However, because it is the non-RWA terms which cause chaos, we calculate the perturbation to the Chirikov pendulum which they cause in lowest order. We obtain a periodically perturbed Chirikov pendulum. This perturbed pendulum is used as a model for the BZT model, and we show that it reproduces the qualitative peculiarities of the power spectra obtained by MAG.

Nonlinear dynamics presents the theorist with a new situation. In the past a theorist would attempt to explain a peculiar spectrum in terms of an analytic expression. In

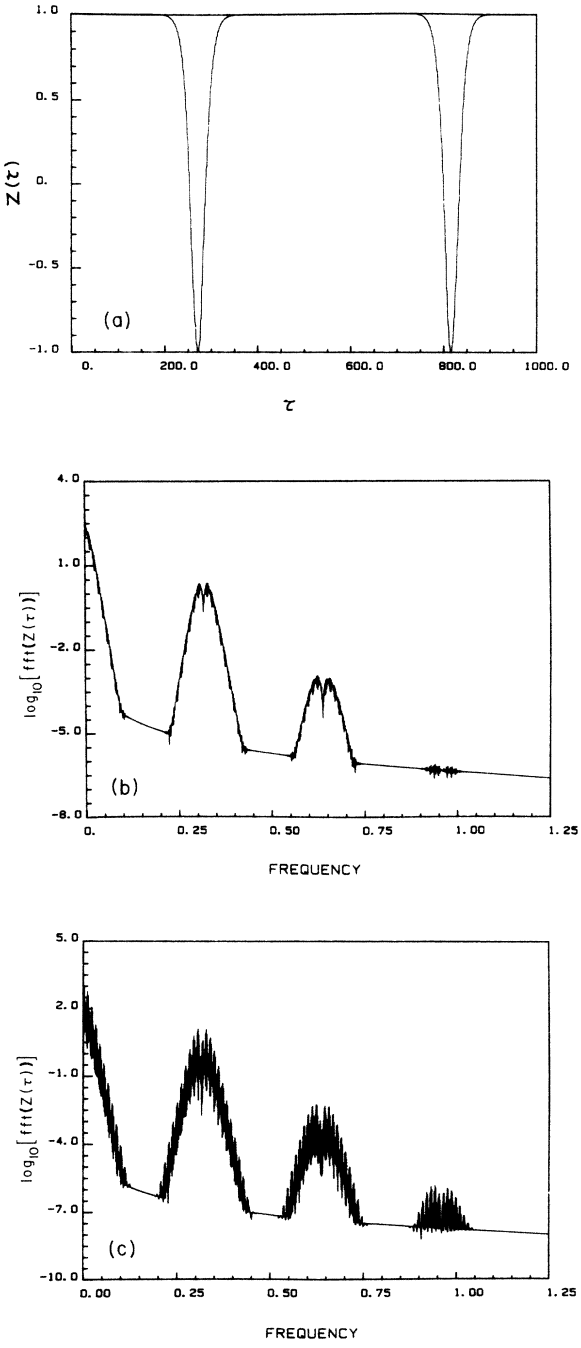

FIG. 1. (a) Numerical results for each figure were obtained from a SUN 2/120 computer in double-precision (14 decimal places). IMSL library routines for solving differential equations and for computing fast Fourier transforms (ftt) were employed. The fft's were computed using a cosine bell window (sine^2). The scaled time τ is used, and the scaling with $N=1$ is also used. This is a plot of $Z(\tau)$ for the MAG model. $\lambda=0.05$, $A(0)=-10^{-5}$, $Z(0)=1$, and $x(0)=y(0)=0$. 100 000 iterations with step size $(\Delta t)=0.05$. 1000 points are plotted. (b) fft for $Z(\tau)$. Log power spectrum is plotted against frequency in hertz (Hz). 10^5 iterations were run but a 4000-point fft was computed from only the first 4000 points, as in Milonni *et al.* (Ref. 4). 1250 points are plotted. (c) fft for $Z(\tau)$. 20 000-point fft from 10^5 iterations with 1250 points plotted. This shows more detailed structure.

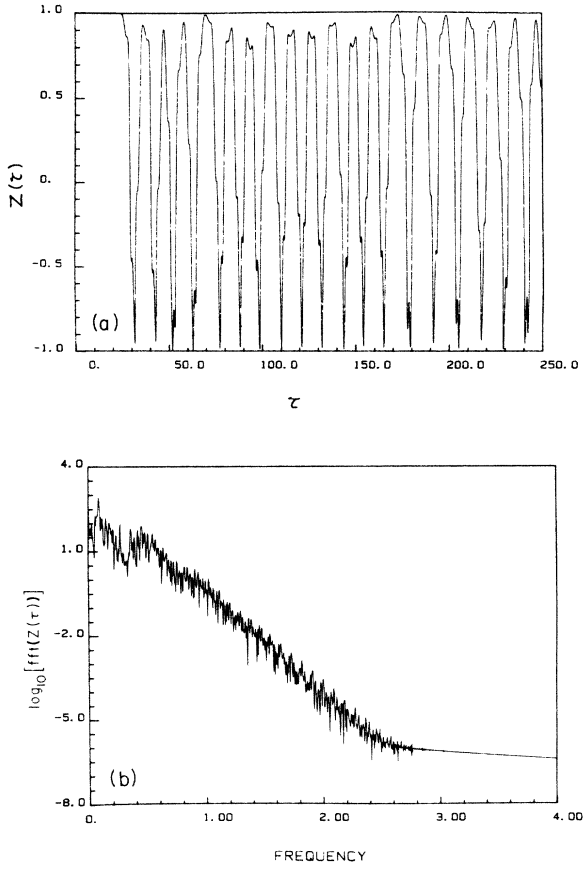

FIG. 2. (a) Plot of $Z(\tau)$. $A(0)=-10^{-6}$, $\lambda=0.5$, $\Delta t=0.05$, 5000 iterations, 1250 points plotted. (b) fft for $Z(\tau)$. 5000-point fft, 1000 points plotted.

the present situation, all we can do is provide an analytic dynamical model, the periodically perturbed pendulum. This model cannot be solved analytically. Nevertheless, we can solve it numerically and thereby show that it does explain the results obtained from our study of the original system. Thus, we find ourselves using a numerical analysis of a simplified model to explain the numerical results of a more complicated model. The gain achieved by this approach is that the simplified model, the periodically perturbed Chirikov pendulum, has been identified as a "universal" basis for chaotic dynamics in diverse physical and mathematical systems.[9,10]

II. TWO-LEVEL QUANTUM SYSTEM IN A RESONANT CAVITY

We consider a two-level quantum system in a resonant cavity. The cavity radiation is dominated by just one mode of the radiation field, which can be tuned to match the level spacing of the two-level system. The presence of the two-level system creates a feedback effect on the radiation field. The Hamiltonian for this system is (see Appendix)

$$H=\tfrac{1}{2}\hbar\omega_0\sigma_z+\hbar\omega(a^\dagger a+\tfrac{1}{2})+\hbar\lambda\sigma_x(a+a^\dagger)\ , \qquad (1)$$

in which Pauli matrices, σ_z and σ_x, have been used to represent the two-level system, and creation-annihilation operators, $a^\dagger$ and a, have been used to represent the radiation field's single mode. The energy separation of the two levels is $\hbar\omega_0$ and the frequency of the radiation mode is ω. Resonant tuning means $\omega_0=\omega$. The strength of the coupling is determined by λ. For a cavity of volume V and a two-level system with electric dipole moment μ, λ is given by[5]

$$\lambda=\left[\frac{2\pi\omega}{\hbar V}\right]\mu^{1/2} . \tag{2}$$

A single two-level system (spin or molecule) in the cavity will not produce the chaos to be described. Instead, N such systems must be present. We restrict N so that it is not so large that these systems interact. For a resonant cavity, such as in a laser, $V=1\text{ m}\times 1\text{ mm}\times 1\text{mm}=1\text{ cm}^3$, and $N<10^{22}$ is acceptable. The frequencies may be anywhere from 10^{15} Hz down to 10^9 Hz. In the former case, we are safe in neglecting dissipative relaxation effects in the two-level systems. In the latter case, such effects may prove important, but we defer consideration of dissipation to a later study. Dissipation in the radiation field (i.e., cavity losses) are negligible in the present context.

III. THE JAYNES-CUMMINGS MODEL AND THE RWA

In the analysis of the dynamics implied by (1), two types of time dependence arise: $\exp[i(\omega_0-\omega)t]$ and $\exp[i(\omega_0+\omega)t]$. The latter term oscillates about zero so rapidly that it is usually acceptable to neglect such terms. This amounts to the RWA. This neglect can be effectuated at the outset by modifying the interaction Hamiltonian in (1)

$$H_I=\hbar\lambda(\sigma_- a^\dagger+\sigma_+ a) , \tag{3}$$

in which $\sigma_\pm=\frac{1}{2}(\sigma_x\pm i\sigma_y)$. With this interaction Hamiltonian in (1), we have the Jaynes-Cummings model[11] at the fully quantum-mechanical level of description. This model is exactly solvable.[12] We will see below how inclusion of the neglected terms converts this integrable model into one exhibiting chaos. A very subtle change in the model results in dramatic dynamical consequences.

The present situation is the reverse of a comparable circumstance in classical physics.[13] The three-particle Toda lattice is integrable and without chaos. However, its low-energy approximation yields the two-particle Henon-Heiles system which does exhibit chaos. In this case, the approximation destroys an extra, conserved quantity; whereas in the Jaynes-Cummings model, an extra, conserved quantity is created by the approximation, as we shall see.

IV. REDUCTION TO CLASSICAL EQUATIONS AND ERROR ESTIMATES

We return to the Hamiltonian (1). The Heisenberg operator equations are

$$\dot\sigma_x=-\omega_0\sigma_y , \tag{4a}$$

$$\dot\sigma_y=\omega_0\sigma_x-2\lambda\sigma_z(a+a^\dagger) , \tag{4b}$$

$$\dot\sigma_z=2\lambda\sigma_y(a+a^\dagger) , \tag{4c}$$

$$\dot a+\dot a^\dagger=-i\omega(a-a^\dagger) , \tag{4d}$$

$$\dot a-\dot a^\dagger=-i\omega(a+a^\dagger)-2i\lambda\sigma_x , \tag{4e}$$

in which a dot denotes a time derivative. These are first-order coupled nonlinear operator equations for an infinite-dimensional Hilbert space. A reduction to coupled ordinary differential equations is achieved by taking expectation values of these operator equations. Define the "classical" variables

$$x=\mathrm{Ex}(\sigma_x) , \tag{5a}$$

$$y=\mathrm{Ex}(\sigma_y) , \tag{5b}$$

$$z=\mathrm{Ex}(\sigma_z) , \tag{5c}$$

$$A=\mathrm{Ex}(a+a^\dagger) , \tag{5d}$$

$$B=\mathrm{Ex}[i(a-a^\dagger)] . \tag{5e}$$

If we assume that expectation values for products factorize, then we get the semiclassical model equations

$$\dot x=-\omega_0 y , \tag{6a}$$

$$\dot y=\omega_0 x-2\lambda Az , \tag{6b}$$

$$\dot z=2\lambda Ay , \tag{6c}$$

$$\dot A=-\omega B , \tag{6d}$$

$$\dot B=\omega A+2N\lambda x , \tag{6e}$$

in which we have included the consequence of having N noninteracting two-level systems. There are two natural second-order equations implicit in (6a)–(6e):

$$\ddot x+\omega_0^2 x=2\omega_0\lambda Az , \tag{7a}$$

$$\ddot A+\omega^2 A=-2N\omega\lambda x . \tag{7b}$$

A comparison with the BZT model[7] shows that the identifications $x\to m$, $z\to n$, $A\to-(\mu/h\lambda)E$, along with (2) and $N/V\to\rho$, make our equations identical with the BZT model which was invoked on purely semiclassical grounds. The MAG model,[4] however, corresponds to these equations with (7b) replaced by

$$\ddot A+\omega^2 A=2N\frac{\lambda}{\omega}\ddot x . \tag{8}$$

At resonance, $\omega=\omega_0$, and using (7a), this yields

$$\ddot A+\omega^2 A=-2N\omega\lambda x+4N\lambda^2 Az , \tag{9}$$

which clearly differs from (7b). The MAG model was also invoked on purely semiclassical grounds, and the source term in (8) may be interpreted as polarization density created by the presence of the two-level system. Equation (7b), however, corresponds with a source term which is an effective current density. As mentioned in the Introduction, this important distinction was emphasized earlier by Mandel.[8] It arises whenever a reduction of a fully quantum-mechanical treatment is made in the manner described here.

How good is the factorization assumption? Given two operators, P and Q, we have assumed that $\mathrm{Ex}(PQ)=\mathrm{Ex}(P)\mathrm{Ex}(Q)$. Generally, this equality is only approximate and $\mathrm{Ex}(PQ)\neq\mathrm{Ex}(P)\mathrm{Ex}(Q)$. In fact, the Schwartz inequality implies

$$\begin{aligned}|\,\mathrm{Ex}(PQ)-\mathrm{Ex}(P)\mathrm{Ex}(Q)\,| &= |\,\mathrm{Ex}\{[P-\mathrm{Ex}(P)][Q-\mathrm{Ex}(Q)]\}\,| \\ &\leq [\,||P-\mathrm{Ex}(P)||\,||Q-\mathrm{Ex}(Q)||\,]^{1/2}\,, \end{aligned} \tag{10}$$

in which $||R||\equiv\mathrm{Ex}(R^{\dagger}R)$ for arbitrary operators P, Q, and R. In getting Eqs. (6) from Eqs. (4), we need estimates for $P=\sigma_y$ and σ_z, and $Q=a+a^{\dagger}$. For these choices of P, we have, say for $P=\sigma_y$,

$$\begin{aligned}||[\sigma_y-\mathrm{Ex}(\sigma_y)]|| &= \mathrm{Ex}[\sigma_0-|\,\mathrm{Ex}(\sigma_y)\,|^2] \\ &\leq \mathrm{Ex}(\sigma_0)=1\,, \end{aligned} \tag{11}$$

in which σ_0 is the 2×2 identity matrix. Thus, for either choice of P, we get

$$\begin{aligned}\mathrm{Ex}[P(a+a^{\dagger})]-\mathrm{Ex}(P)\mathrm{Ex}(a+a^{\dagger}) &\leq \{\,||[(a+a^{\dagger})-\mathrm{Ex}(a+a^{\dagger})]||\,\}^{1/2} \\ &= \{\mathrm{Ex}[(a+a^{\dagger})^2]-[\mathrm{Ex}(a+a^{\dagger})]^2\}^{1/2} \\ &= O(1/2\sqrt{n}\,)\,. \end{aligned} \tag{12}$$

Since the size of $\mathrm{Ex}(PQ)$ here is $O(\sqrt{n}\,)$, the relative error is $O(1/n)$. For a continuous laser, a single cavity mode will have roughly 10^{10} photons present,[14] i.e., $n=10^{10}$. In our studies, this means we make an error in z of less than 10^{-5}. In pulsed mode,[14] $n\sim10^{18}$ can be achieved for steady-state times of nanoseconds, yielding errors less than 10^{-13}.

The system of Eqs. (6a)—(6e) also admits two conserved quantities. These are

$$x^2+y^2+z^2=C_1\,, \tag{13a}$$

$$\frac{\omega}{4}(A^2+B^2)+\frac{N}{2}\omega_0 z+N\lambda Ax=C_2\,. \tag{13b}$$

Therefore, we have five coupled first-order equations with two conserved quantities. This is equivalent to three coupled first-order equations, which is just enough for the possibility of chaos.[15]

V. THE RESULTS OF NUMERICAL SIMULATIONS

The numerical simulations are run for the resonant case, $\omega=\omega_0$, with $\omega_0=10^{15}$ Hz. To accommodate this large frequency, we work in a scaled dimensionless time, $\tau=\omega_0 t$. For initial conditions, $x(0)=y(0)=0$, $z(0)=1$, $B(0)=0$, and $A(0)$ is chosen so that $-2\lambda A(0)=10^{-6}$, in order to agree with the MAG-model calculations. Let $\beta=4\lambda^2N$. The MAG model was originally run for $\beta=0.01$ and $\beta=1.0$. Because we have to preset the product $\lambda A(0)$, we are free to scale things so that $N=1$ and $\lambda=0.05$ and $\lambda=0.5$ for $\beta=0.01$ and $\beta=1.0$, respectively. Thus, each simulation is run for the scaled time τ with scaled values $N=1$ and $\lambda=0.05$ or 0.5. Figures 1 and 2 exhibit the results for the MAG model. The time course

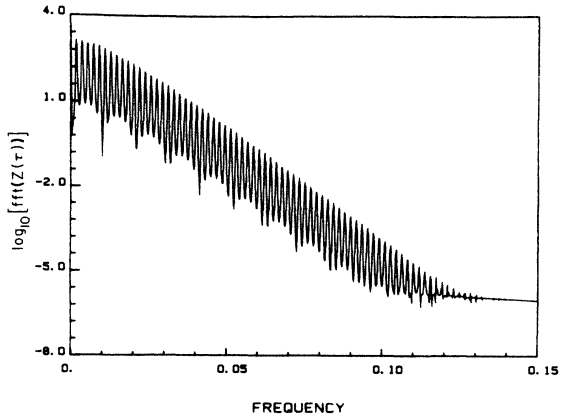

FIG. 3. 20000-point fft for $Z(\tau)$ in MAG model. 750 points are plotted. This is an enlargement of the initial shoulder by about eight fold. The fundamental at 0.0018 Hz, and many harmonics are apparent.

for $z(\tau)$ is shown as well as its log power spectrum. In Fig. 1, $\lambda=0.05$, and the period of oscillation is approximately 550τ. This yields a fundamental frequency of 0.0018. The scale of the power spectrum abscissa is only 1 Hz in the scaled time. The fundamental frequency is in the extreme left in the peak next to the zero ordinate. Figure 3 shows the fundamental frequency clearly on an enlargement of the initial portion of the spectrum. The other two large peaks in Fig. 1 occur at approximately 178 and 356 times this fundamental. There is also a structure at about 533 times the fundamental. These appear to be simple harmonics of the frequency 0.32 Hz. There is also a curious depression at the tops of these peaks. Figures 4 and 5 show enlargements of these secondary peaks. It is clear that they are quite regular on a fine scale. In Fig. 2, $\lambda=0.5$, and there is a fundamental period of about 11.5τ, with a frequency of 0.087. This frequency appears in the spectrum as a sharp spike near the zero ordinate on an almost linear decay of over eight decades. Figure 6 shows an enlargement of the initial portion of this spectrum, and clearly exhibits its irregular

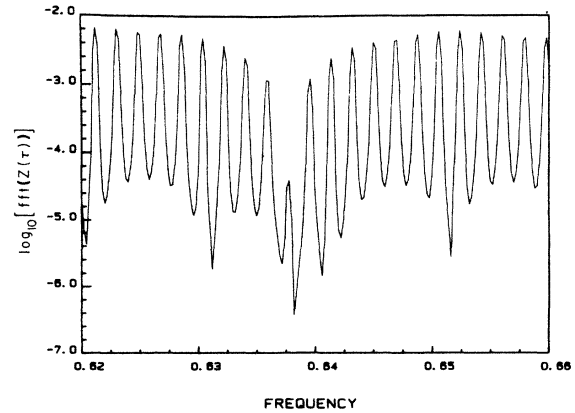

FIG. 4. 20000-point fft over 10^5 iterations. Enlargement of the peak around 0.64 Hz in Fig. 1(c).

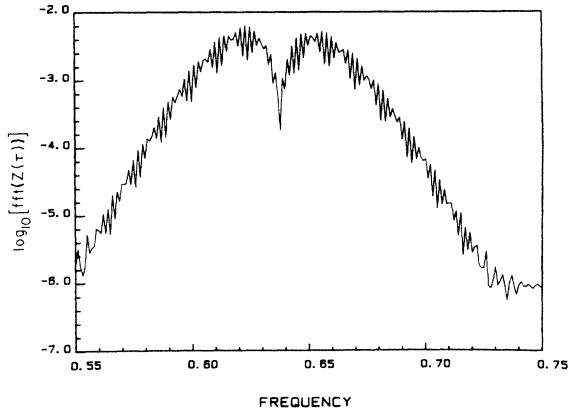

FIG. 5. 4000-point fft over 4000 iterations. Enlargement of the peak around 0.64 Hz in Fig. 1(b).

nature on a fine scale, as well as the peak at frequency 0.087.

In Figs. 7 and 8 we exhibit comparable results for the BZT model which we have derived. There is a close similarity between the results for $\lambda=0.05$ and the corresponding results for the MAG model. This is a result of the small difference between Eqs. (7b) and (9) for small values. However, the $\lambda=0.5$ results show the difference between these two models. The BZT chaotic spectrum cuts off earlier than does the MAG spectrum, and has a larger negative slope.

Liapunov exponents have been computed for each case as well. The results for $\lambda=0.05$ are that the maximum Liapunov exponent is 0.03 for both models. Indeed, the computation procedure[16] indicates that the value is converging on zero as $\lambda\to 0$. For $\lambda=0.5$, the maximum Liapunov exponent is 0.080 for the MAG model, and is 0.196 for the BZT model; a clear confirmation of the exponential separation of initially close trajectories as observed for the BZT model,[7] and of the apparently noisy, continuous spectrum observed for the MAG model.[4] In Fig. 9 we show one spike from the $z(\tau)$ profile seen in Fig. 1, or equivalently in Fig. 7. This spike has been enlarged so that a small scale modulation can be seen. It is precisely this modulation which shows up in the power spectrum at frequency 0.32 Hz.

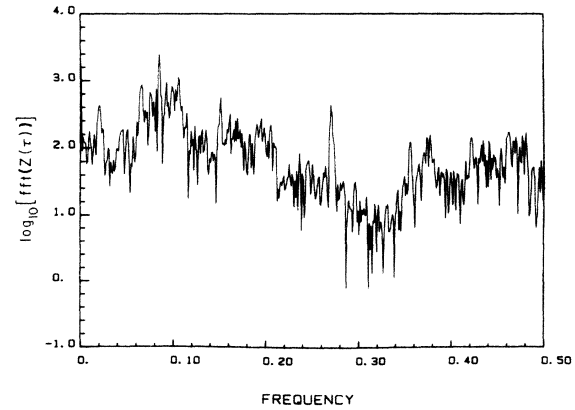

FIG. 6. Same as Fig. 2(b) enlarged eightfold. The peak at 0.087 is clear.

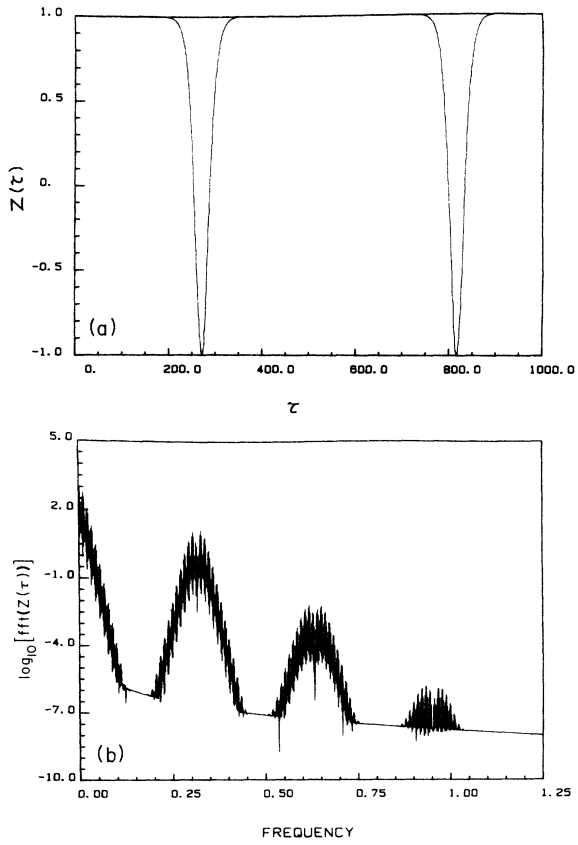

FIG. 7. (a) $Z(\tau)$ for BZT model. $\lambda=0.05$, $A(0)=-10^{-5}$, and all other conditions identical with Fig. 1(a). (b) fft for $Z(\tau)$ in BZT model. 20 000-point fft over 10^5 iterations. 1250 points are plotted.

VI. THE EBERLY-CHIRIKOV PENDULUM

The analysis performed by Belobrov *et al.*[7] did not involve spectra or Liapunov exponents. They looked at phase-space trajectories instead. In fact they observed the effect of positive Liapunov exponents in the exponential separation of initially close trajectories. Their phase-space description involved a change of variables, which we also find useful.

Equations (7) strongly suggest effective action-angle variables:

$$A=\left[\frac{I}{\omega}\right]^{1/2}\cos\phi,\quad \dot{A}=-\sqrt{I\omega}\sin\phi(=-\omega B)\,, \tag{14a}$$

$$x=\left[\frac{J}{\omega_0}\right]^{1/2}\cos\theta,\quad \dot{x}=-(J\omega_0)^{1/2}\sin\theta(=-\omega_0 y)\,, \tag{14b}$$

$$I=\omega(A^2+B^2),\quad J=\omega_0(x^2+y^2)\,, \tag{14c}$$

$$\phi=\arctan\left[\frac{B}{A}\right],\quad \theta=\arctan\left[\frac{y}{x}\right]. \tag{14d}$$

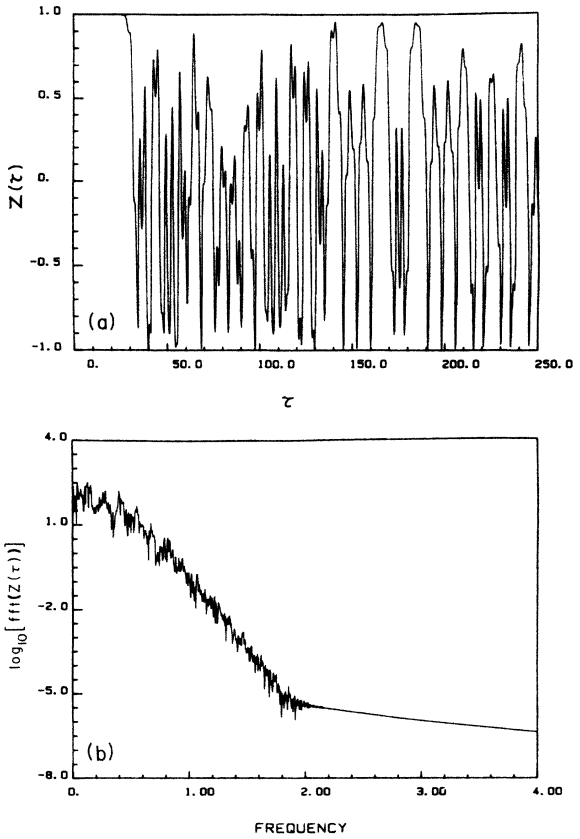

FIG. 8. (a) $Z(\tau)$ for BZT model. $\lambda=0.5$, $A(0)=-10^{-6}$, and all other conditions identical with Fig. 2(b). The cutoff is earlier than in Fig. 2(b), and the details differ. (b) fft for $Z(\tau)$ in (a). Compare with Figs. 2(a) and 2(b).

With these changes, Eqs. (6) become

$$\dot{I}=4\omega N\lambda\left[\frac{IJ}{\omega\omega_0}\right]^{1/2}\cos\theta\sin\phi\ , \tag{15a}$$

$$\dot{\phi}=\omega+2N\lambda\left[\frac{\omega J}{I\omega_0}\right]^{1/2}\cos\phi\cos\theta\ , \tag{15b}$$

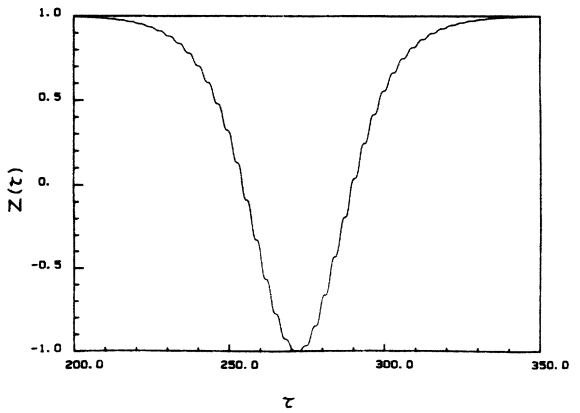

FIG. 9. $Z(\tau)$ spike for BZT model with conditions identical with Fig. 1(a). Note high-frequency modulations in this enlargement.

$$\dot{J}=-4\omega_0\lambda z\left[\frac{IJ}{\omega\omega_0}\right]^{1/2}\cos\phi\sin\theta\ , \tag{15c}$$

$$\dot{\theta}=\omega_0-2\lambda z\left[\frac{I\omega_0}{\omega J}\right]^{1/2}\cos\phi\cos\theta\ , \tag{15d}$$

$$\dot{z}=2\lambda\left[\frac{IJ}{\omega\omega_0}\right]^{1/2}\cos\phi\sin\theta\ . \tag{15e}$$

The conserved quantities, C_1 and C_2 of Eqs. (13), can be rewritten after multiplication by ω_0^2 and 4ω, respectively:

$$G=J\omega_0+\omega_0^2z^2\ , \tag{16a}$$

$$H=I\omega+2N\omega\omega_0z+4\omega N\lambda\left[\frac{IJ}{\omega\omega_0}\right]^{1/2}\cos\phi\cos\theta\ . \tag{16b}$$

Clearly, $\dot{G}=\dot{H}=0$. The RWA suggests the further change of variables,

$$\psi=\phi-\theta\ , \tag{17a}$$

$$\eta=\phi+\theta\ , \tag{17b}$$

$$\sin\phi\cos\theta=\tfrac{1}{2}(\sin\psi+\sin\eta)\ , \tag{17c}$$

$$\cos\phi\cos\theta=\tfrac{1}{2}(\cos\psi+\cos\eta)\ , \tag{17d}$$

$$\cos\phi\sin\theta=\tfrac{1}{2}(-\sin\psi+\sin\eta)\ . \tag{17e}$$

This variable change converts (15a)—(15e) into

$$\dot{I}=2\omega N\lambda\left[\frac{IJ}{\omega\omega_0}\right]^{1/2}(\sin\psi+\sin\eta)\ , \tag{18a}$$

$$\dot{\psi}=\omega-\omega_0+\left[N\lambda\left[\frac{\omega J}{I\omega_0}\right]^{1/2}+\lambda z\left[\frac{I\omega_0}{\omega J}\right]\right]^{1/2}(\cos\psi+\cos\eta)\ , \tag{18b}$$

$$\dot{J}=2\omega_0\lambda z\left[\frac{IJ}{\omega\omega_0}\right]^{1/2}(\sin\psi-\sin\eta)\ , \tag{18c}$$

$$\dot{\eta}=\omega+\omega_0+\left[N\lambda\left[\frac{\omega J}{I\omega_0}\right]^{1/2}-\lambda z\left[\frac{I\omega_0}{\omega J}\right]^{1/2}\right](\cos\psi+\cos\eta)\ , \tag{18d}$$

$$\dot{z}=-\left[\frac{IJ}{\omega\omega_0}\right]^{1/2}(\sin\psi-\sin\eta)\ . \tag{18e}$$

The two conserved quantities could now be used to eliminate J and η in favor of z, ψ, and I. This is precisely the approach of Belobrov *et al.*[7] Moreover, the RWA amounts to omitting all η terms, which decouples η from the remaining variables. Thus, in the RWA, elimination of J by (16a) produces three coupled equations in z, ψ, and I plus one conserved quantity. This means that in the RWA we really have a two-variable problem, and no chaos is possible.[15]

We can go even further with the RWA. Define the quantity P by

$$P=\sqrt{IJ}\cos\psi\ . \tag{19}$$

Consequently,

$$\dot{P}=(\omega_0-\omega)\sqrt{IJ}\sin\psi+N\lambda\left[\frac{\omega}{\omega_0}\right]^{1/2}J\sin[2(\eta-\psi)]$$
$$-\lambda z\left[\frac{\omega_0}{\omega}\right]^{1/2}I\sin[2(\psi+\eta)]\ . \tag{20}$$

In the RWA, and at resonance ($\omega=\omega_0$), we have $\dot{P}=0$, i.e., an extra conserved quantity. We may now write

$$\dot{I}=2N\lambda\sqrt{IJ}\sin\psi\ , \tag{21a}$$

$$\dot{J}=2\lambda z\sqrt{IJ}\sin\psi\ , \tag{21b}$$

$$\dot{\psi}=\left[N\lambda\left[\frac{J}{I}\right]^{1/2}+\lambda z\left[\frac{I}{J}\right]^{1/2}\right]\cos\psi\ , \tag{21c}$$

$$\dot{z}=-\frac{\lambda}{\omega}\sqrt{IJ}\sin\psi\ , \tag{21d}$$

$$G=J\omega+\omega^2z^2\ , \tag{21e}$$

$$H=I\omega+2N\omega^2z+2N\lambda P\ , \tag{21f}$$

$$P=\sqrt{IJ}\cos\psi\ , \tag{21g}$$

$$\dot{G}=\dot{H}=\dot{P}=0\ . \tag{21h}$$

At $t=0$, $J(0)=0$, and $z(0)=1$ implies $G=\omega^2$. Therefore we have for all t

$$J=\omega(1-z^2)\ . \tag{22}$$

Eberly's analysis[1] suggests one final change of variables. Set

$$z=\cos\rho\ , \tag{23a}$$

$$\dot{z}=-\sin\rho\,\dot{\rho}\ , \tag{23b}$$

$$\ddot{z}=-\cos\rho\,\dot{\rho}^2-\sin\rho\,\ddot{\rho}\ . \tag{23c}$$

It is easy to verify from (21a)–(21g) that

$$\ddot{z}=-\frac{N\lambda^2}{\omega}J-\frac{\lambda^2z}{\omega}I\ . \tag{24}$$

Using (21f), (22), (23c), and (24) yields

$$-\cos\rho\,\dot{\rho}^2-\sin\rho\,\ddot{\rho}$$
$$=-N\lambda^2\sin^2\rho$$
$$-\frac{\lambda^2}{\omega}\left[\frac{H-2N\lambda P}{\omega}\cos\rho-2N\omega\cos^2\rho\right]\ . \tag{25}$$

Using (21d), (21g), (21h), and (23b) yields

$$-\cos\rho\,\dot{\rho}^2=-\frac{\lambda^2}{\omega}\left[\frac{H-2N\lambda P}{\omega}\cos\rho-2N\omega\cos^2\rho\right]$$
$$+\frac{\lambda^2P^2}{\omega^2\sin^2\rho}\cos\rho\ . \tag{26}$$

Together with (25), this implies Eberly's spherical pendulum equation

$$\ddot{\rho}=N\lambda^2\sin\rho+\frac{\lambda^2P^2}{\omega^2\sin^3\rho}\cos\rho\ . \tag{27}$$

Note that ρ is measured from the vertical, spherical polar axis. This equation follows from an effective Hamiltonian

$$H_\rho=\tfrac{1}{2}P_\rho^2+N\lambda^2\cos\rho+\frac{\lambda^2P^2}{2\omega^2\sin^2\rho} \tag{28}$$

in which $P_\rho=\dot{\rho}$.

The constant P is not arbitrary. $J(0)=0$ implies $P=0$ for all t. Therefore, the spherical pendulum reduces to Chirikov's planar-pendulum equation

$$\ddot{\rho}=N\lambda^2\sin\rho\ . \tag{29}$$

The right-hand side has its origin in the feedback effect of the two-level system on the radiation, as given by (7b). The initial condition $z(0)=1$ implies $\rho(0)=0$, but it is not so simple in this representation to deduce $\dot{\rho}(0)$. Let us return to Eq. (24) and use equations (21e) and (21f). In equation (21f), set $P=0$ and note that $z(0)=1$ and $I(0)=\omega A^2(0)$ which imply $H=\omega^2A^2(0)+2N\omega^2$. Therefore, we get

$$\ddot{z}=-N\lambda^2(1+3z)(1-z)-\lambda^2A^2(0)z \tag{30}$$

with the effective Hamiltonian

$$H_z=\tfrac{1}{2}P_z^2+N\lambda^2(z+z^2-z^3)+\tfrac{1}{2}\lambda^2A^2(0)z^2\ , \tag{31}$$

where $P_z=\dot{z}$. We know from (21d) that $z(0)=0$ because $J(0)=0$. Therefore, $H_z=N\lambda^2+\frac{1}{2}\lambda^2A^2(0)$, and we have

$$\dot{z}=\sqrt{2}\{(1-z^2)[N\lambda^2+\tfrac{1}{2}\lambda^2A^2(0)-N\lambda^2z]\}^{1/2}\ . \tag{32}$$

Equations (23a)–(23b) together with (32) imply

$$\dot{\rho}=-\sqrt{2}[N\lambda^2+\tfrac{1}{2}\lambda^2A^2(0)-N\lambda^2\cos\rho]^{1/2}\ , \tag{33}$$

from which we deduce $\dot{\rho}(0)=-\lambda\,|\,A(0)\,|$. Therefore, the Chirikov pendulum of Eq. (29) has initial conditions: $\rho(0)=0$ and $\dot{\rho}(0)=-\lambda\,|\,A(0)\,|$. For sufficiently small $\lambda A(0)$, this corresponds with near-separatrix motion. It is perturbed near-separatrix motion which can be chaotic.[9,10]

VII. NON-RWA PERTURBATIONS

The unperturbed Chirikov pendulum cannot be chaotic.[15] Let us look for the corrections to Eq. (29) resulting from inclusion of η terms neglected in the RWA. From equation (18e) we have

$$\ddot{z}=-\frac{\lambda}{\omega}\frac{1}{2}\left[\left[\frac{J}{I}\right]^{1/2}\dot{I}+\left[\frac{I}{J}\right]^{1/2}\dot{J}\right]\sin\psi$$
$$-\frac{\lambda}{\omega}\sqrt{IJ}\,(\cos\psi\,\dot{\psi}-\cos\eta\,\dot{\eta})\ . \tag{34}$$

Since we seek corrections to the RWA, keep Eqs. (21a)–(21c) and also use

$$\dot{\eta}=2\omega+\left[N\lambda\left[\frac{J}{I}\right]^{1/2}-\lambda z\left[\frac{I}{J}\right]^{1/2}\right]\cos\psi\ . \tag{35}$$

Substituting these equations into (34) yields

$$\ddot{z}=-N\frac{\lambda^2}{\omega}J(1-\cos\psi\cos\eta)-\frac{\lambda^2}{\omega}zI(1+\cos\psi\cos\eta)$$
$$+2\lambda\sqrt{IJ}\cos\eta\ . \tag{36}$$

Using Eqs. (23a)–(23c) and (21d) gives

$$\dot{\rho}=\frac{\lambda}{\omega}\sqrt{I\omega}\sin\psi\ , \tag{37a}$$

and

$$-(\cos\rho)\dot{\rho}^2=-(\cos\rho)\frac{\lambda^2}{\omega^2}I\omega\sin^2\psi\ . \tag{37b}$$

Therefore, Eq. (36) can be rewritten as

$$-\ddot{\rho}\sin\rho=-N\lambda^2(\sin^2\rho)(1-\cos\psi\cos\eta)$$
$$-\frac{\lambda^2}{\omega^2}(\cos\rho)I(1+\cos\psi\cos\eta-\sin^2\psi)$$
$$+2\lambda\sqrt{IJ}\cos\eta\ . \tag{38}$$

Now, the I term on the right-hand side corresponds with the azimuthal angular momentum of a spherical pendulum, so that a restriction to the planar pendulum of the RWA amounts to the substitution: $\cos\psi\sim-\cos\eta$. While this eliminates the I term, it creates a coefficient of $1+\cos^2\eta$ for the first term on the right-hand side of (38). Its time average over the short times associated with the fast frequency of the η term yields the periodically perturbed Chirikov pendulum equation

$$\ddot{\rho}=\tfrac{3}{2}N\lambda^2\sin\rho-2\lambda\omega[A^2(0)+2N(1-\cos\rho)]^{1/2}\cos\eta\ , \tag{39}$$

in which $\eta=2\omega t$ is taken and $I\sim\omega A^2(0)+2N\omega(1-z)$ has been used in accord with equation (21f) and the RWA value for I. The initial conditions remain $\rho(0)=0$ and $\dot{\rho}(0)=-\lambda\,|\,A(0)\,|$. Thus, Eq. (39) describes a periodically perturbed, pendulum motion.

Equation (39) does not possess an analytic solution. However, numerical simulation can be used to show that it does provide a good quantitative model for the spectral behavior of the original BZT (or MAG) model. For $\lambda=0.05$, we obtain the results in Fig. 10 which clearly show the important, previously unexplained features of the spectrum obtained by MAG (Ref. 4). Recall that for $\lambda=0.05$ the MAG and BZT models are in close agree-

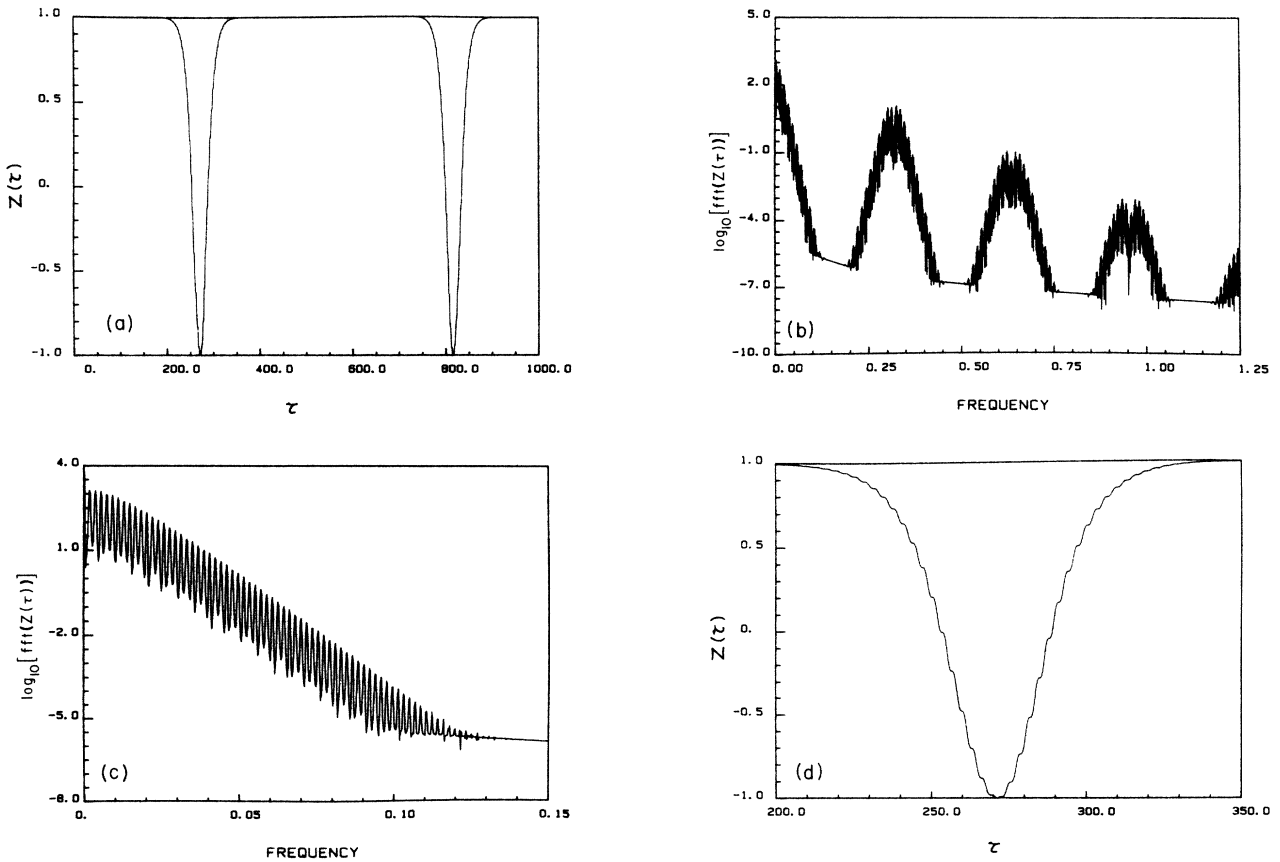

FIG. 10. (a) Perturbed Chirikov pendulum for $\lambda=0.05$ and conditions appropriate to Fig. 1(a). (b) fft for $Z(\tau)=\cos\rho(\tau)$. Compare with Figs. 1(c) and 7(b). (c) Initial peak of fft enlargement. Compare with Fig. 3. (d) Enlargement of first spike in (a). Compare with Fig. 9.

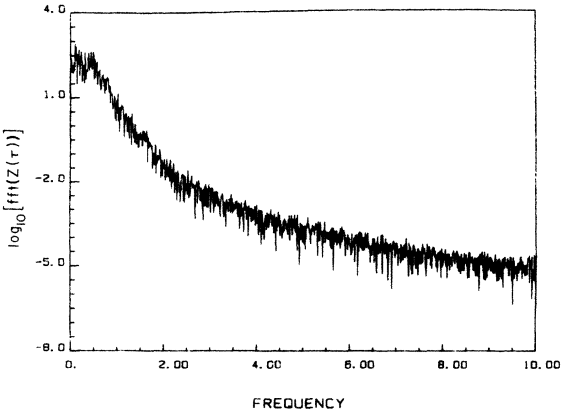

FIG. 11. Same as in Fig. 10 except $\lambda=0.5$. fft for $Z(\tau)$.

ment. It is now clear that the modulation seen in Fig. 9, which is responsible for the secondary peaks in the spectrum in Figs. 1(b) and 7(b), is a result of the non-RWA term $2\omega t$. This corresponds with a frequency of $2\omega/2\pi=1/\pi=0.318$ Hz, precisely as is observed in the figures. The other peaks are merely harmonics of this fundamental perturbing frequency.

For $\lambda=0.5$, we do not believe that Eq. (39) properly includes all of the η dependence. Nevertheless, Fig. 11 shows that it does produce a spectrum in qualitative agreement with the BZT model. If we instead run Eq. (29) with initial conditions $\rho(0)=0$ and $\dot{\rho}(0)=0$, so that we are precisely on the separatrix, then round-off error provides a source of noise, and Fig. 12 shows the resulting spectrum. This figure was determined by using only single precision, which is of order 10^{-7}, in the computations, as compared with using double precision in all the other figures. Right away this generates an effective $\dot{\rho}$ of about 10^{-7}, so that when Fig. 12 is compared with Fig. 2(b) for the MAG model, there is close correspondence. Thus, the shape of the spectrum in the chaotic regime is explained as that due to noisy separatrix motion of a Chirikov pendulum.

It is possible to change the initial conditions

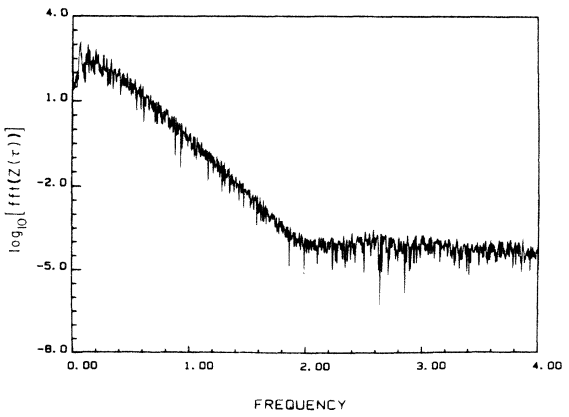

FIG. 12. Noisy separatrix motion of pendulum. fft of $\cos\rho(\tau)$.

$x(0)=y(0)=0$ so that $J(0)\neq 0$ and $P\neq 0$ in the RWA. In this case, we will get a periodically perturbed Eberly pendulum for small λ. We have not yet explored this case in sufficient detail to report on it here.

VIII. DISCUSSION OF RESULTS

Starting with the purely quantum-mechanical problem posed by the Hamiltonian in (1) we have shown how to derive the BZT model for the interaction of a two-level system with a cavity-mode radiation field. The derivation required on expectation-value factorization, for which an error estimate was made. The RWA treatment of this model was shown to contain an Eberly spherical pendulum, which reduced to a Chirikov planar pendulum when the special initial conditions used in this study were imposed. The effects on this pendulum resulting from inclusion of non-RWA terms present in the full model were shown to be given by a periodically perturbed Chirikov pendulum. This model of a model explained the peculiar nature of the power spectra observed for the MAG and BZT models.

The indication of chaos suggested by the power spectrum for $\lambda=0.5$ was confirmed by computing a positive Liapunov exponent for the MAG and BZT models. A positive Liapunov exponent is also obtained for $\lambda=0.05$, and for any λ, for that matter. This is consistent with the near-separatrix motion of a periodically perturbed Chirikov pendulum. We conclude that the BZT model possesses genuine chaos, and our model of the model by a periodically perturbed pendulum explains the origin of chaos in this system. It remains to determine whether or not this chaos reflects bona fide chaos in the quantum system with which we began our study.

The first difficulty we meet is with the definition of "quantum chaos." Several definitions exist and their interconnections have not yet been fully elucidated. Three main views follow.

(1) Quantum chaos refers to the appearance of chaos in the time evolution of a dynamical variable, i.e., expectation value of a Heisenberg observable. The chaos referred to in the preceding sentence is that observed and well studied in classical chaos or ordinary coupled first-order differential equations. It's tools are power spectra and Liapunov exponents. This definition is directly connected to classical chaos by Ehrenfest's theorem and the classical limit.

(2) Quantum chaos refers to a property of the eigenspectrum. Specifically, a transition in spectral type occurs which is the analogue to classical chaos (as used above). Our model is in clear opposition to this; our model's spectrum is set once and for all at the outset. Special initial conditions ($P=0$) lead to the possibility of near separatrix motion in a Chirikov pendulum. For all other initial conditions ($P\neq 0$), there is a centrifugal barrier to near separatrix motion, and thus to chaos in the motion. Consequently, with the same eigenspectrum but with differing initial conditions we do or do not get chaos.

(3) Quantum chaos refers to a property of the Schrödinger wave function, that it is somehow chaotic in the classical sense. We have adopted this view inadver-

tently in so far as one accepts that expectation values for Heisenberg observables are directly connected with Schrödinger wave functions.

It is known that a finite bounded quantum system cannot exhibit chaos; it is at worst quasiperiodic.[17] Even a c-number periodically driven finite quantum system does not appear to exhibit chaos even though it develops a continuous spectrum. We believe that neither of these cases applies to our example. Our problem involves an infinite-dimensional Hilbert space (because of the photons) and we are looking at the projected behavior of this system given by $\mathrm{Ex}(\sigma_z)$. We recognize that our treatment is effectively semiclassical (a result of expectation factorization), and we realize that even subtle changes can create dramatic artifacts.

Return to Eqs. (6). There are two conservation laws, (13a) and (13b). This leaves three independent variables. This is the minimum number of variables which can exhibit classical chaos. Whether they do or not depends on subtle changes. For example, if $\omega_0=0$ is used in (6a)—(6e) along with $x(0)=0$, then (y,z) become a parametrically perturbed harmonic oscillator, perturbed by A, an autonomous harmonic oscillator. This case exhibits no chaos and can be expressed analytically in closed form in terms of functions such as $\cos[2(\lambda/\omega)A(0)\cos(\omega t)]$. Now suppose $\omega_0\neq 0$ and $N=0$, so that there is no x feedback to A. This is still a variety of parametrically perturbed harmonic oscillator. The coupling of the simple (x,y) harmonic oscillator through the common variable y makes this problem mathematically complicated. Technically, we say that analytic expressions for the solutions require the use of "time-ordered exponentials." In this case it is the noncommutativity of 3×3 matrices needed to express the solutions as ordered exponentials which causes difficulty. We do not believe that this case shows chaos and are concluding a parallel numerical analysis to show this. If this proves to be so, then a chance at chaos occurs only after $N\neq 0$ is chosen, and a simple linear x feedback to A is allowed. It is clear from the unique appearance of N in Eq. (6e) that this is the term giving rise to the $\sin(\rho)$ term in Eqs. (29) and (39). Without it, there is no pendulum, and consequently, no opportunity for chaotic, periodically perturbed, near-separatrix motion. (The reader is cautioned not to confuse this pendulum in a Bloch-Maxwell system with another pendulum in a Bloch-Maxwell system, the famous hyperbolic secant pulse of McCall and Hahn.[18])

The relationship between the three-particle Toda lattice and the two-particle Henon-Heiles system is an example of this subtlety for a classical system. The relationship between our quantum system in (1) and the Jaynes-Cummings model which uses the interaction Hamiltonian in (3) is an example of this subtlety for a quantum system (the Jaynes-Cummings model is exactly integrable). It could be said that we introduced chaos through the factorization step. However, we prefer to believe, until it is clearly shown to be wrong, that our observations reflect a genuine quantum chaos present in the purely quantum-level description,[19] and that this chaos is in part a consequence of a finite-dimensional projection of an infinite-dimensional dynamics. In this system this projection exhibits chaos because the system effectively contains a perturbed, planar, near-separatrix-motion pendulum. As was observed below Eq. (29) above, this pendulum has its origin in the modification of the cavity-radiation field caused by feedback from the state of the two-level system.

The question of the existence of quantum chaos needs to be embedded into the following sequence: classical, semiclassical, and fully quantal. It is clear that the semiclassical treatment of quantum phenomena, such as given by Eqs. (6), can exhibit chaos. They are equivalent to a kind of classical dynamical system in five variables with two conservation laws. This was clearly demonstrated in complementary ways by BZT (Ref. 7) and MAG (Ref. 4), although not until now has the mechanism for these observations been proposed. The investigation of a purely quantal treatment is mathematically demanding, and we are still looking at this aspect of the problem. We repeat that the eigenspectrum per se is not enough because of the essential dependence on initial conditions instead.

We believe that bona fide chaos in a quantum system arises from the intrinsically nonlinear coupling of particle states and radiation fields, which is absent in both Schrödinger equations for particle states in externally prescribed electromagnetic fields, and field equations for radiation fields produced by externally prescribed sources. Within the framework of second-quantized-field theories, the simplest setting for this potentiality is the Dirac-Maxwell coupled-field theory. In essence, we have presented a nonrelativistic, non-second-quantized version of such coupling in the present paper. The presence of the resonant cavity is essential for the manifestation of chaos resulting from the nonlinear coupling. The chaos we have seen here is a property of the combined quantum system made up of two-level system, radiation field, and resonant cavity.

ACKNOWLEDGMENTS

We are indebted to R. Roy for invaluable discussions throughout the pursuit of these studies. We are especially appreciative of his bringing to our attention Refs. 1 and 8. We thank Tony Yu for helping us set up our computer approach to the numerical studies. We thank Joe Ford for informative discussions of related perspectives, and thank G. Casati for providing a copy of a report of his work prior to publication. This work was supported by National Science Foundation Grant No. PHY-85-42492.

APPENDIX

If we include all of the electromagnetic terms appropriate in a nonrelativistic treatment, then we get for the electric dipole approximation the Hamiltonian

$$H=\tfrac{1}{2}\hbar\omega_0\sigma_z+\hbar\omega(a^\dagger a+\tfrac{1}{2})+\hbar\lambda\sigma_x(a+a^\dagger)+\hbar\beta[a^2+(a^\dagger)^2+aa^\dagger+a^\dagger a]\ . \tag{A1}$$

This can be rewritten suggestively in the form

$$H=\tfrac{1}{2}\hbar\omega_0\sigma_z+\hbar(\omega+2\beta)(a^\dagger a+\tfrac{1}{2})+\hbar\lambda\sigma_x(a+a^\dagger)+\hbar\beta[a^2+(a^\dagger)^2]\ . \tag{A2}$$

The Heisenberg equations (4a)—(4c) remain unchanged when (A2) is used. However, Eqs. (4d) and (4e) are modified and yield the equation

$$\ddot{a}+\ddot{a}^{\dagger}=-\omega(\omega+2\beta)(a+a^{\dagger})-2\omega\lambda\sigma_x \ . \tag{A3}$$

Introduce the parameters

$$\omega'=\sqrt{\omega(\omega+4\beta)} \ \text{ and } \ \lambda'=\frac{\omega}{\omega'}\lambda \ . \tag{A4}$$

Instead of (4a)—(4e) we get

$$\dot{\sigma}_x=-\omega_0\sigma_y \ , \tag{A5a}$$

$$\dot{\sigma}_y=\omega_0\sigma_x-2\left[1+\frac{4\beta}{\omega}\right]^{1/2}\lambda'(a+a^{\dagger})\sigma_z \ , \tag{A5b}$$

$$\dot{\sigma}_z=2\left[1+\frac{4\beta}{\omega}\right]^{1/2}\lambda'(a+a^{\dagger})\sigma_y \ , \tag{A5c}$$

$$\ddot{a}+\ddot{a}^{\dagger}=-(\omega')^2(a+a^{\dagger})-2\omega'\lambda'\sigma_x \ . \tag{A5d}$$

Under the conditions for our studies, $n=10^{10}$ protons with $\omega=10^{15}$ sec^{-1} and $\lambda=2\times10^{8}$ sec^{-1} with $\beta=10^{-1}$ sec^{-1}. Consequently, $\sqrt{1+4\beta/\omega}\cong1+2\times10^{-16}$. Therefore, to within an error less than one part in 10^{15}, we may neglect the $\sqrt{1+4\beta/\omega}$ in Eqs. (A5a)—(A5d) which leaves the system equivalent to Eqs. (4a)—(4e) when the primes are dropped.

[1]J. H. Eberly, Phys. Lett. **26A**, 499 (1968).

[2]B. V. Chirikov, Doctoral thesis, Novosibirsk State University, Novosibirsk (1970).

[3]G. M. Zaslavskii and B. V. Chirikov, Usp. Fiz. Nauk **105**, 3 (1971) [Sov. Phys.—Usp. **14**, 549 (1972)].

[4]P. W. Milonni, J. R. Ackerhalt, and H. W. Galbraith, Phys. Rev. Lett. **50**, 966 (1983); **51**, 1108(E) (1983).

[5]E. T. Jaynes and F. W. Cummings, Proc. IEEE **51**, 89 (1963).

[6]P. W. Milonni, J. R. Ackerhalt, and H. W. Galbraith, Ref. 4.

[7]P. I. Belobrov, G. M. Zaslavskii, and G. Kh. Tartakovskii, Zh. Eksp. Teor. Fiz. **71**, 1799 (1977) [Sov. Phys.—JETP **44**, 945 (1977)].

[8]L. Mandel, Phys. Rev. A **20**, 1590 (1979).

[9]A. J. Lichtenberg and M. A. Lieberman, *Regular and Stochastic Motion* (Springer-Verlag, New York, 1983), Chap. 2.

[10]B. V. Chirikov, Phys. Rep. **52**, 265 (1979).

[11]J. H. Eberly, N. B. Narozhny, and J. J. Sanchez-Mondragon, Phys. Rev. Lett. **44**, 1323 (1980); N. B. Narozhny, J. J. Sanchez-Mondragon, and J. H. Eberly, Phys. Rev. A **23**, 236 (1981).

[12]J. R. Ackerhalt, Ph.D thesis, University of Rochester (1974).

[13]A. J. Lichtenberg and M. A. Lieberman, Ref. 9, Chap. 1.

[14]R. Loudon, *The Quantum Theory of Light*, 2nd ed. (Oxford, New York, 1983), p. 21.

[15]A. J. Lichtenberg and M. A. Lieberman, Ref. 9, p. 383.

[16]G. Benettin, L. Galgani, and J. M. Strelcyn, Phys. Rev. A **14**, 2338 (1976); G. Benettin and L. Galgani, J. Stat. Phys. **27**, 153 (1982).

[17]G. Casati, in *Quantum Probability and Applications II*, edited by L. Accardi (Springer-Verlag, Heidelberg, 1985).

[18]S. L. McCall and E. L. Hahn, Phys. Rev. **183**, 457 (1969); see L. Allen and J. Eberly, *Optical Resonance and Two-Level Atoms* (Wiley, New York, 1975), pp. 82—83.

[19]M. Kus, Phys. Rev. Lett. **54**, 1343 (1985). This is closely related but involves a different definition of quantum chaos, and other approximations.